FINAL TECHNICAL REPORT

Paleoseismic Investigation of the Portland Hills fault near Clackamas, Oregon:

United States Geological Survey Award Number 03HQGR0020

Mark A. Hemphill-Haley
Department of Geology
Humboldt State University
Arcata, CA 95521
mark@humboldt.edu

Technical support for this project provided by

Lee M. Liberty
Center for Geophysical Investigation of the Shallow Subsurface
Boise State University
lml@cgiss.boisestate.edu

Ian P. Madin
Oregon Department of Geology and Mineral Industries
800 NE Oregon Street #28, Suite 965
Portland, OR 97232
ian.p.madin@state.or.us

Research Supported by the U.S. Geological Survey (USGS), Department of the Interior, under USGS award number 03HQGR0020. The views and conclusions contained in this document are those of the authors and should not be interpreted as necessarily representing the official policies, either expressed or implied, of the U.S Government.

TABLE OF CONTENTS

INTRODUCTION

The Portland, Oregon, and Vancouver, Washington, metropolitan area is located in a seismically active region (Figure 1). Geological and geophysical studies indicate that potentially active faults, including the Portland Hills, East Bank, Oatfield, and Frontal faults, are located in the immediate vicinity of downtown Portland and Vancouver, an urban corridor with a population of nearly 2 million people (e.g., Blakely et al. 2004, Blakely et al., 1995; Pratt et al., 2001; Wong et al., 2000; Wong et al., 2001). Little is known about the earthquake potential and structural style of these faults. The lack of information regarding fault activity lies largely in the absence of geomorphic expression of the faults. . The present topography is due, largely, to three factors. First, 16.9 - 6 Ma Columbia River flood-basalt (CRB) flows blanketed the region and created a regionally extensive, relatively flat volcanic terrain (Yeats et al., 1996). Second, the topography was again reconstructed during the 12-15 ka Missoula flood events (Waitt, 1985 REF), where upwards of 40 catastrophic flood events reworked and deposited up to 30 m of sediments regionally. Finally, urbanization continues to alter and mask any surface topographic expression of the faults. The identification of active faulting is further complicated by probable right-lateral, strike-slip displacement of the northwest-striking faults that dominate the region (Beeson et al., 1985; Beeson and Tolan, 1990; Beeson et al., 1989; Yelin and Patton, 1991). Faults that have dominantly lateral displacement will tend to minimize any post-Missoula flood relief that may be associated with surface rupture or deformation. The lack of a geomorphic expression, extensive modern surface deposits, strike-slip displacement, and urbanization makes hazard assessment difficult using typical geologic mapping methods. Measuring fault displacement by correlating changing lithologies within nearby water wells was useful (Hemphill-Haley et al., 2001), but was limited due to the poorly-defined boundary that separates modern deposits from reworked older sediments and the large variability in sediment types that comprise modern deposits. Large-scale geophysical methods (e.g., aeromagnetics, industry-scale seismic) are useful to locate faults (Blakely et al., 2006, Blakely et al., 2000), but do not provide the information needed to evaluate present-day earthquake hazards.

In previous investigations (Liberty et al., 2003, Hemphill-Haley et al. (2000, 2001) Madin and Hemphill-Haley (2001), Wong et al., 2001) we used subsurface mapping using high-resolution geophysical methods to locate potential near surface faults and associated deformed sediments in order to better assess the neotectonic history of this region. The success from using high-resolution geophysics combined with neotectonic studies in the Portland Basin is largely due to the presence of a hard basalt basement, of known age, within a few hundred meters of the ground surface that has strong magnetization, and large seismic impedance contrasts compared to overlying sediments. The sediments largely consist of interbedded fine- and coarse-grained deposits associated with the Missoula flood deposits. The varying lithology within the sedimentary section provided numerous seismic boundaries to image.

The purpose of this investigation was to utilize information gathered from our previous NEHRP-funded studies, in addition to other available data, to locate and excavate a trench across a portion of the Portland Hills fault (PHF). It was our intention to use this trench information to

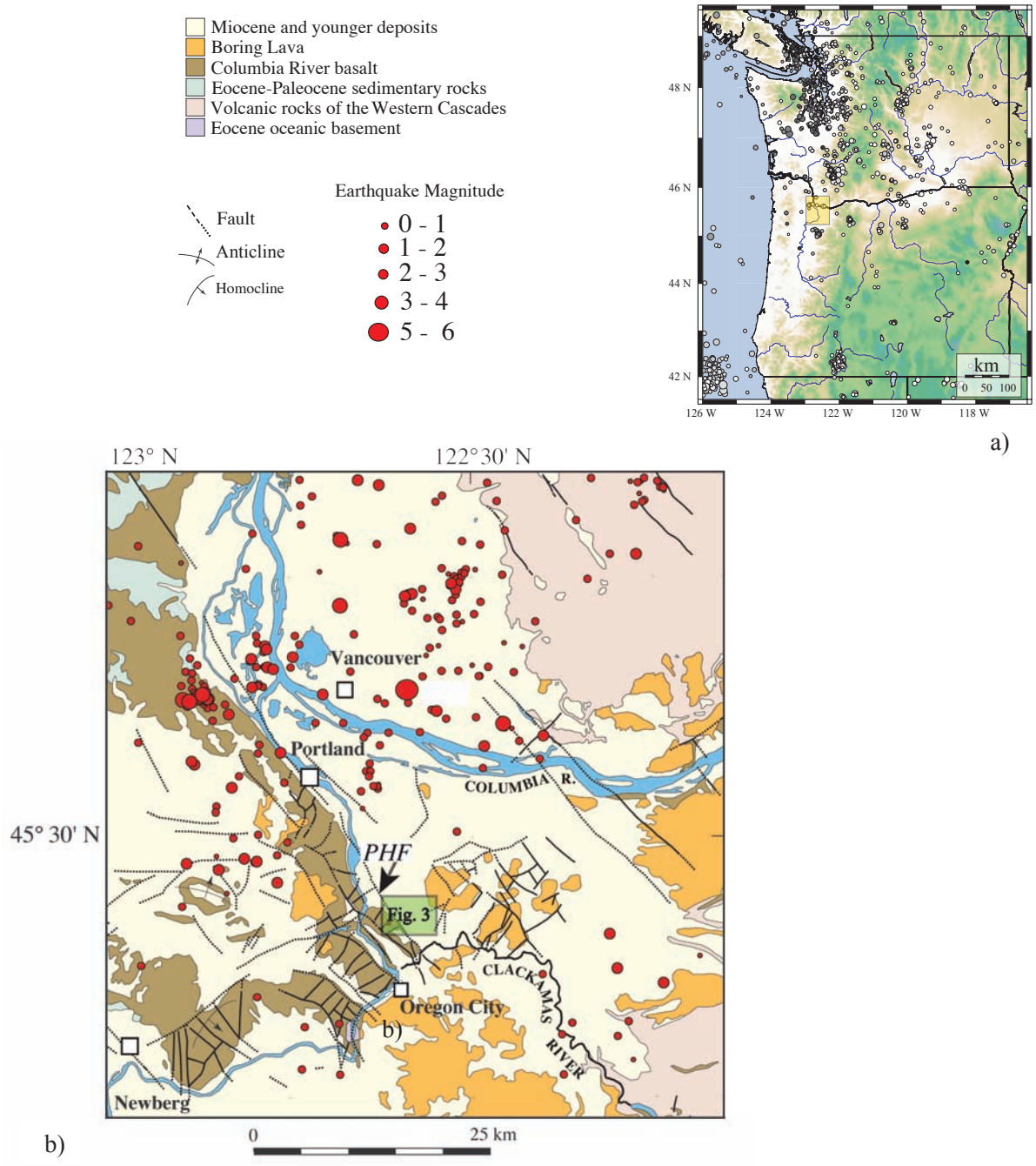

Figure 1 - a) Historical seismicity of the Pacific Northwest since 1973. Circles represent earthquake epicenters , b) Portland metropolitan area with historical seismicity since 1841. Figure from Wong et al. (2001).

assess whether the fault has had Quaternary surface rupture and possibly multiple Quaternary rupture events.

PREVIOUS INVESTIGATIONS

Earthquake hazards studies in western Oregon and Washington often rely on geophysical methods to identify the location and characteristics of crustal faults, since a pronounced topographic expression from faulting does not necessarily appear on the surface (e.g., Blakely et al., 1995; Johnson et al., 1999). The absence of pronounced surficial features typically considered indicative of high slip rate fault activity, such as alluvial scarps, offset and aligned drainages and tonal, vegetation lineaments, does not preclude this fault from being a significant seismic source. Instead this can be attributed to surficial deposits that consist of modern flood sediments, a considerable amount of urban development, and the possibility that a significant portion of lateral slip occurs on the fault. Numerous industry seismic reflection surveys in the region were acquired in the past exploring for oil and gas deposits. Published results from these surveys (e.g.,Werner et al., 1992) document vertical offsets in the basement rocks and suggest that younger sediments are also offset. Regional aeromagnetic studies (Blakely et al., 2000; Blakely et al., 1995) have identified lineaments that correlate with crustal faults, including the PHF. Blakely et al. (1995) identified a magnetic lineament associated with the PHF as a long-wavelength dominated signal to the east separating a short-wavelength dominated signal that appears to the west. Recent regional seismic reflection surveys that have focused on neotectonic studies (e.g., Liberty et al., 1999; Pratt et al., 2001; Wong et al., 2001) document offsets in Plio-Pleistocene age sediments above basement rocks. Prior to this study, Holocene-age disruption of sediments in the Portland metropolitan area was inferred, but not directly documented with geophysical studies and trenching.

The PHF had been identified and located only on the basis of large-scale geomorphic features such as the asymmetric anticline and fault line escarpment of the Portland Hills (Madin, 1990), from an aeromagnetic survey (Blakely et al., 1995), and from local well logs.

As part of two previous U.S. Geological Survey National Earthquake Hazards Reduction Program grants (USGS Award Number 00HQGR0023 01HQPA0002) we employed multiple geophysical methods, including high-resolution seismic reflection, ground penetrating radar (GPR), and magnetic profiling to locate the Portland Hills fault at North Clackamas Park (NCP) and Rowe Middle School (RMS) south of Portland (Figure 2). We also incorporated data from nearby water-wells to correlate the geophysical data and help direct the emplacement of the seismic profiles.

North Clackamas Park site

The investigation at the NCP site consisted of conducting two high-resolution seismic surveys to provide detailed images of the upper 100 m of the stratigraphic section. They enabled us to locate significant offset in the Miocene-age Columbia River basalts (CRB) and overlying sediments. We also developed ground magnetic profiles along the seismic transects to correlate with offset and orientation in the volcanic basement, or CRB's. Seismic, magnetics, and well log information indicate that basalts and younger sediments which we interpreted as

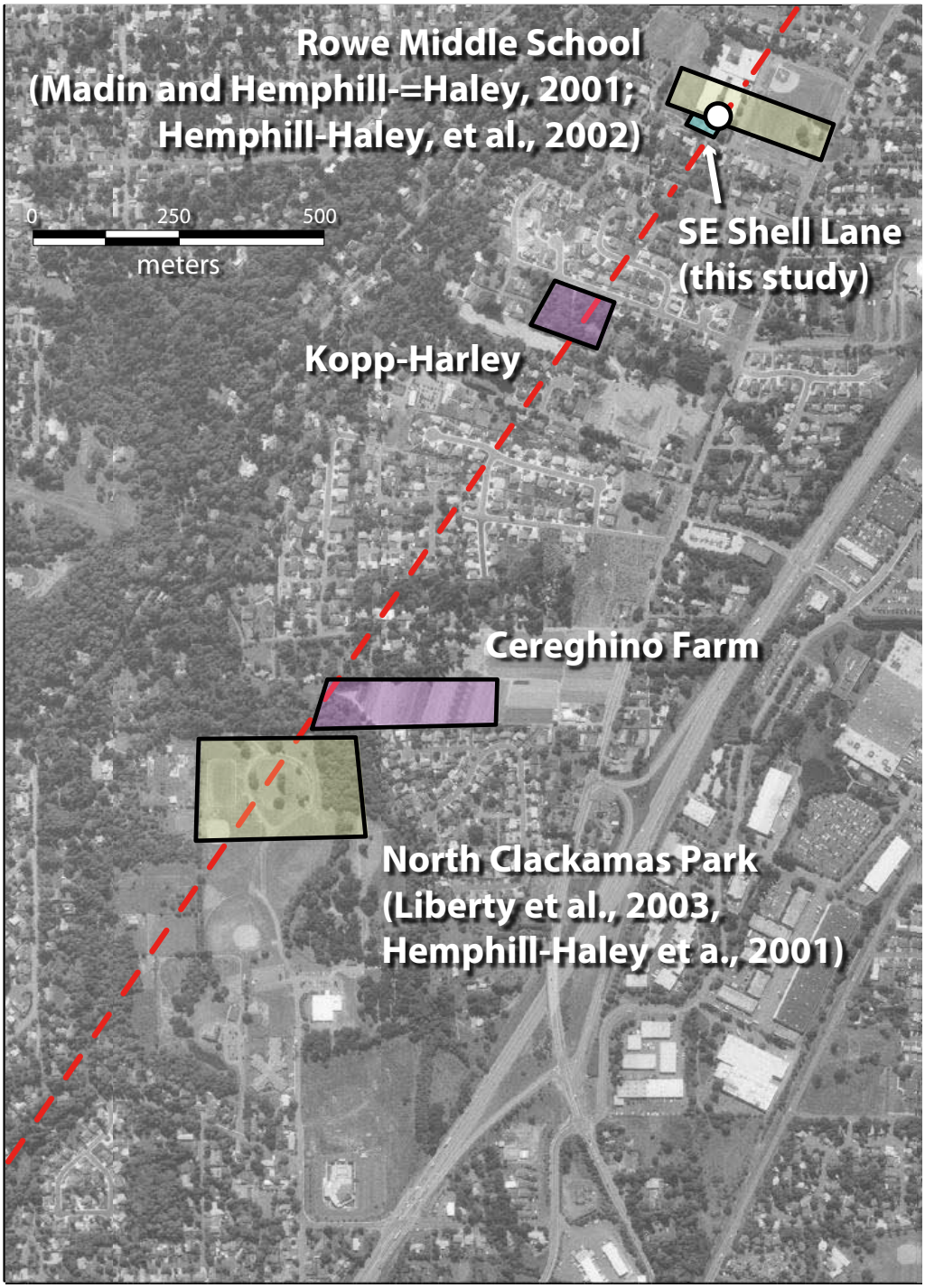

Figure 2 - Locations of potential trench sites that include two geophysical study sites, North Clackamas Park and Rowe Middle School (yellow quadrilaterals) and three undeveloped parcels along the projection of the Portland Hills fault between the two geophysical sites, Cereghino farm and Kopp-Harley parcels (violet quadrilaterals) and SE Shell Lane (blue quadrilateral). The inferred trace of the Portland Hills fault (dashed line) is located on the basis of results from information from both NEHRP investigations. The location of the Rowe School side-hill excavation is depicted as an open circle.

Pleistocene Missoula flood deposits, dip steeply to the east. The dipping strata were imaged to within about 10 m below the land surface.

We interpreted these data to represent a major splay of the Portland Hills fault that offsets post-CRB sediments. The change from flat lying CRB and younger sediments to relatively steep-dipping strata provided an indication of the fault location. The data did not provide equivocal evidence for the style of deformation. However, the position of the offset CRB markers is consistent with a southwest-dipping reverse fault which places the Portland Hills northeastward over the adjacent basin.

Based on that study we were able to demonstrate that post-CRB sediments are faulted. We concluded that, if the youngest faulted sediments imaged from the high-resolution seismic reflection methods are Missoula-flood related deposits, then there has been at least one episode of coseismic surface rupture in the past 15,000 to 12,000 years.

Rowe Middle School Site

We conducted an investigation during NEHRP USGS Award Number 01HQPA0002 to further characterize the Portland Hills fault and locate a potential site to locate Holocene deformation along the PHF near NCP. As a result, we identified an active construction site approximately 1.5 km from NCP along the inferred strike (Figures 2 and 3) at Rowe Middle School. The site had adequate open space for a geophysical survey. An engineering borehole

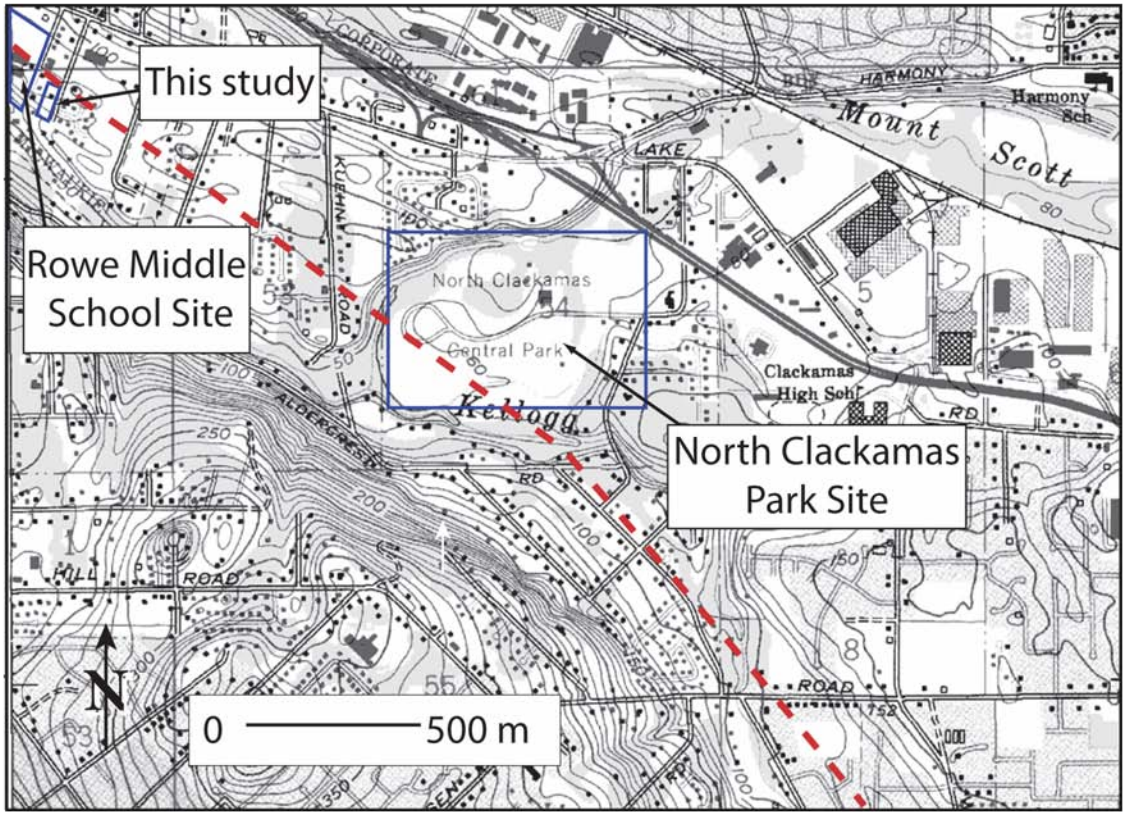

Figure 3 – Topography of southern Portland Hills fault study sites. North Clackamas site (Hemphill-Haley et al., 2000), Rowe Middle School site (Hemphill-Haley et al. 2001) and this study (SE Shell Lane). Approximate location of the Portland Hills fault (red dashed line) is based on regional aeromagnetics, (Blakely et al., 1995), geophysical locations (Liberty et al., 1999), and an excavation exposure at Rowe Middle School (Madin and Hemphill-Haley, 2001; Wong et al., 2003)

(B-4) at RMS (schematically represented in Figure 4) shows unsaturated silty sands to sandy gravels in the upper 11 m of the section, with a clay aquatard at the base of the sand sequence. The sedimentary sequence from the borehole is consistent with Missoula flood deposits.

A retaining wall excavation along the eastern boundary of the school revealed folded, fractured and faulted sediments. We identified seven rhythmites, or flood events (Missoula flood deposits) that exhibit more than one meter of shortening over the 36 m long trench (Figure 4, Madin and Hemphill-Haley, 2001). The exposure, including an approximately 1 m-deep trench, exposed several deformed horizons that truncate against an anticline. We also interpreted that sediments above this unconformity are folded suggesting that two separate shortening events occurred within the flood deposit sequence (Madin and Hemphill-Haley, 2001). We were able to occupy the side-hill exposure only for a brief period of time due to construction constraints. Therefore, were unable to conduct a detailed paleoseismic investigation. We did conclude, however, that the deformation likely represented multiple Quaternary deformation events.

We conducted several geophysical investigations at RMS parallel and adjacent to the backfilled trench that included a ground-based magnetic survey, multiple frequency (50 and 100 MHz) GPR surveys, and a high-resolution seismic survey to focus on the deformation within the top 20 m of the site (Figures 4, 5 and 6). We extended the surveys beyond the length of the side-hill excavation in order to attempt to correlate the geophysical results and deformation observed from NCP to that observed in the trench.

The magnetic survey suggested a topographic expression occurs on the CRB/sediment boundary at RMS that is similar to that observed at NCP and that the deformation beneath the trench is likely similar to the deformation observed at NCP.

GPR results from a 100 MHz sources provided a pattern of reflections that mimic the trench log with imaging depths up to 2.5 m (Figure 4b). A 50 MHz profile resulted in a similar pattern of deformation to 5 m depth (Figure 4c). The form of the folds, expressed by the dipping reflections, represent an anticlinal and synclinal pair. The hinge of the buried portion of the anticline appeared more sharp-crested than the exposed sediments indicated possibly indicating the presence of a fault at depth. The surface exposure log provided evidence for at least one meter of shortening along the length of the trench while the GPR profiles clearly suggest a greater amount is present along the longer geophysical transects

To extend the imaging depth and extent of the GPR data acquired at the RMS site, we also acquired a high-resolution seismic reflection survey to image the top 20 m of the sediment section (Figures 4d and 5). The 150 m-long seismic profile shows a strong reflection section from 1 to 15 m depth that mimic both the GPR and trench results. Several folds appear at depth along the transect and deformation extends beyond the length of the trench. The geophysical images suggest deformation that we logged from the temporary trench does not represent the complete strain history of the PHF.

GEOLOGIC SETTING

Earthquakes in the Pacific Northwest (Figure 1a) occur due to intraplate and interplate stresses related to both active subduction of the Juan de Fuca plate along the Cascadia subduction zone and large-scale crustal block rotations within the North American plate (Wells et al., 1998). Although the largest earthquakes (M 8 or larger) occur along the subduction zone and smaller,

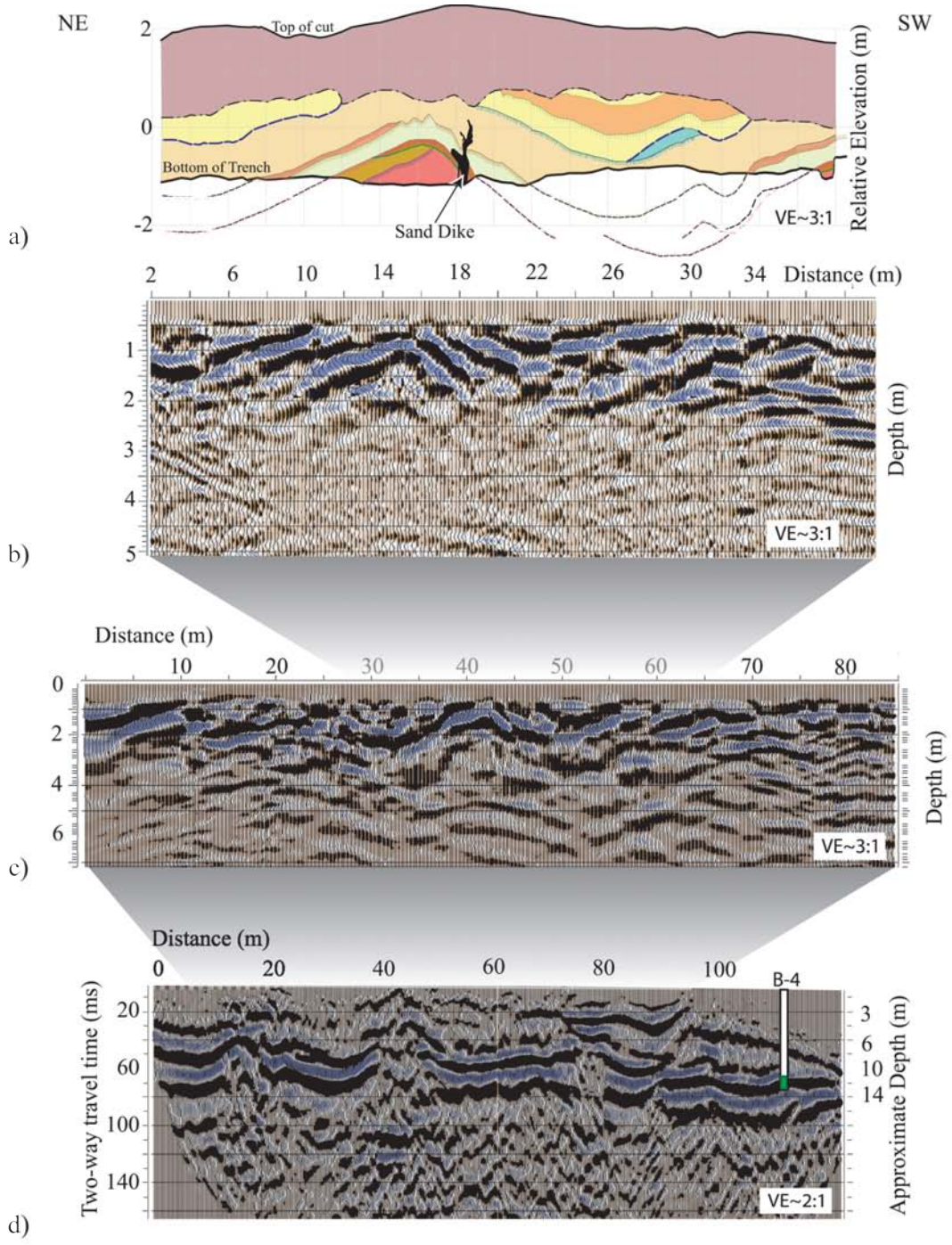

Figure 4 - Rowe Middle School site geological and geophysical investigation results. a) sketch log of sidehill excavation at construction site along southeast side of school (see Figure 2c). b) 100 Mhz Ground Penetrating Radar survey profile. c) 50 Mhz Ground Penetrating Radar survey profile. d) High-resolution seismic reflection profile.

deep earthquakes occur within the Juan de Fuca plate (e.g., the 2000 Nisqually earthquake), a significant hazard also exists from earthquakes in the upper crust of the North American plate (Wong, 1997). Upper plate earthquakes occur on crustal faults at relatively shallow depths (< 25 km) and are of particular concern to the populated areas of western Oregon and Washington, where northwest-trending crustal faults have formed as a result of the breakup and rotation of the Cascade fore arc (Wells et al., 1998; Blakely et al., 2000). Crustal faults are known to exist beneath most of the densely populated regions of western Oregon and Washington, and because of their shallow depth, crustal earthquakes can produce severe ground shaking (Wong et al., 2000).

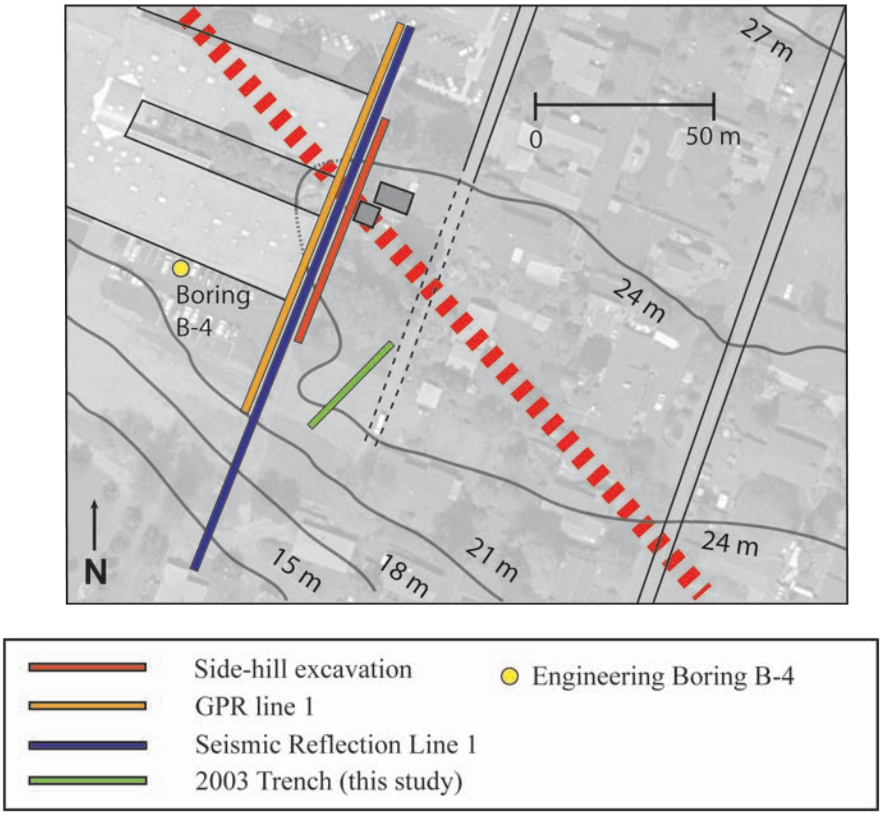

Figure 5 - Aerial photograph of the Rowe Middle School and site indicating locations of geophysical lines, side-hill excavation, Portland Hills fault (dashed red line).

The Portland area (Figure 1b) is the most seismically active region in Oregon in historical times . Based on the 150-year historic record, six earthquakes of Richter magnitude (M_L) 5 or greater have occurred within the metropolitan area including the damaging 1962 M_L 5 Portland and 1993 M_L 5.6 Scotts Mills earthquakes (Bott and Wong, 1993), the latter causing $30 million in damage to buildings and infrastructure in a mainly rural setting (Madin et al., 1993). An earthquake similar to the Scotts Mills sequence in downtown Portland could be devastating.

The Portland Basin (Figure 1b) contains more than 500 m of Miocene age fine-grained sediments, Pliocene-Pleistocene age coarse-grained deposits, and late Pleistocene to Recent age (12-15 ka) coarse- and fine-grained channel fill and overbank flood deposits (Swanson et al.,

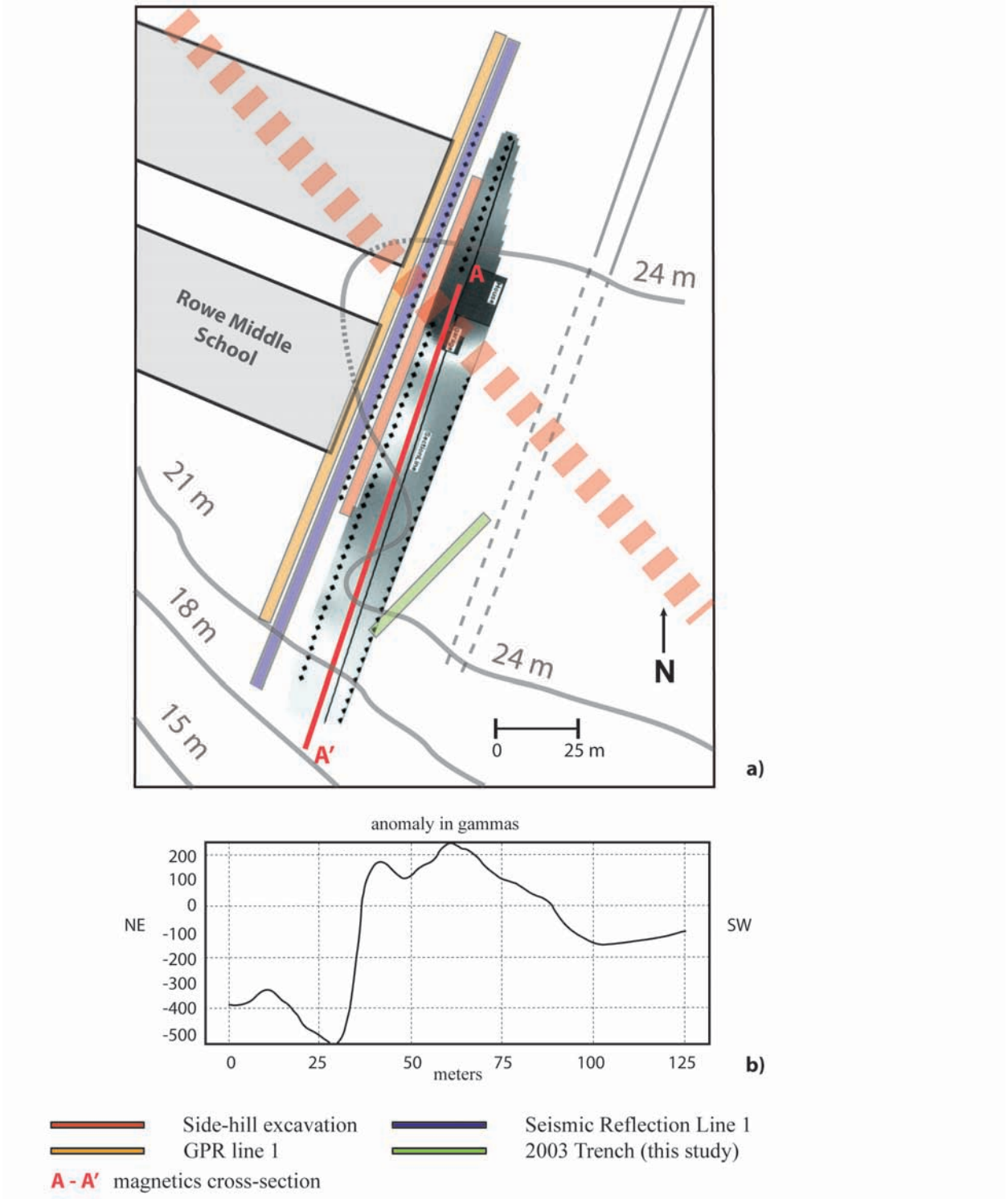

Figure 6 - Grid map with location of magnetic data points (black diamonds) (Hemphill-Haley et al., 2001) with respect to sidehill excavation, other geophysical surveys and trench (this study). Strong anomaly coincides with pronounced fold observed in excavation (Figure 6). b) Cross-section of magnetic grid map. Shows sharp and relatively high-amplitude (~700 gamma) anomaly.

1993; Yeats et al., 1996) associated with the draining of glacial Lake Missoula (Waitt, 1985). The Missoula deposits are low velocity and may amplify ground shaking in the Portland Metropolitan area during a large earthquake (Pratt et al., 2001). Beneath the sedimentary cover, the stratigraphic section is dominated by Miocene and older volcanic and sedimentary units.

The Portland Basin lies at the boundary between two crustal blocks that separate a compressional volcanic arc regime to the north and an extensional arc to the south (Magill et al., 1981; Wells, 1990); the basin may have formed in response to the transfer of strain between the basin bounding faults (Beeson et al., 1985; Yelin and Patton, 1991). The basin is controlled by northwest-striking faults that, on the basis of geologic relations, earthquake focal mechanisms, and potential field anomalies, have right-lateral, strike-slip displacement (Beeson et al., 1985; Beeson and Tolan, 1990; Beeson et al., 1989; Blakely et al., 1995; Blakely et al., 2000; Yelin and Patton, 1991;). The northeast boundary of the Portland Basin is controlled by the Sandy River and Frontal faults (Blakely et al., 1995; Walsh et al., 1987; Yelin and Patton, 1991). The southwest boundary of the Portland Basin is controlled by the Portland Hills Fault (PHF) and perhaps also by the Oatfield and East Bank faults (Beeson et al., 1991; Blakely et al., 1995; Wong et al., 2001).

Three crustal faults that define the southwest boundary of the Portland Basin have been identified as potential sources for damaging crustal earthquakes of M_L 6 or larger in the Portland region (Wong et al., 2000). An evaluation of earthquake recurrence based on the historical record suggests that crustal earthquakes of M_L 6 or larger occur somewhere in the Portland region on average about every 1000-2000 years (Bott and Wong, 1993). Wong et al. (2000) showed that earthquakes from local faults present a greater hazard than earthquakes associated with the Cascadia subduction zone. The PHF, extending through downtown Portland, has been identified as the greatest local hazard (Wong et al., 2000). In a moment magnitude (M_w) 6.8 earthquake scenario on the PHF, calculated ground motions, as characterized by peak horizontal acceleration, exceeded 1g. Thus, although in its 150-year existence the Portland metropolitan area has gone relatively unscathed by damaging earthquakes, strong ground shaking generated by an earthquake on the PHF or nearby fault will have a major impact on the Portland area.

APPROACH

Trench Site Selection

To date, our investigation has focused primarily on the southern part of the PHF which is less urbanized, traverses low-lying areas away from the contemporary Willamette River and maintains a strong aeromagnetic signature (Figure 1). Based on information gathered during the previous two NEHRP-funded studies we considered potential trench sites located between our two prior investigation sites (Figures 2 and 3), the North Clackamas Park site (Hemphill-Haley et al., 2001) and the Rowe Middle School site (Hemphill-Haley et al. 2002). We considered these two sites to provide the best constraint on the location of the fault because it was imaged well in the offset of CRB basement and distorted younger beds. Because of the density of urbanization and the lack of geomorphic expression of the fault we focused on relatively large, undeveloped parcels of land between the two study sites that cross the projection of the fault and might afford us opportunities for exploration (Figure 2).

Based on our evaluation of the two geophysical study sites, NCP and RMS, we did not consider them to be potentially useful paleoseismic investigation sites. Specifically, NCP had been strongly modified by earth moving equipment and had a shallow groundwater level that would even pose problems in the summer. Additionally, the deformation zone at that location was sufficiently broad that an exploratory trench of several hundred meters might be required to define the fault. Likewise, the RMS site was unsuitable mainly because of building locations and lack of unmodified materials available for trenching.

We initially selected three potential sites for trenching excluding NCP and RMS (Figure 2). They are the Cereghino Farm property, Kopp-Harley property and a small undeveloped lot at SE Shell Lane adjacent to the RMS site. We conducted a shallow seismic reflection survey along an E-W transect at the Cereghino Farm site.

The results led us to the conclusion that the fault was likely located west of the property or just at its western end at a location that would be unsuitable for trenching. The Kopp-Harley property, was sufficiently distant from the two well-constrained locations (NCP and RMS) that there were large uncertainties in the approximate location of the fault. The property was flat-lying with no geomorphic expression of the fault. It became evident that the uncertainty was substantial enough at this location that we may completely miss the fault if we trenched only where there was sufficient open ground for the excavation.

We concluded that the SE Shell Lane property would be suitable for several reasons. First, it is located directly adjacent to the southern margin of the RMS property. The side-hill excavation was located at the property line shared by RMS and the SE Shell Lane parcel. Results from the geophysical surveys (Figure 4 and 5) suggested that the zone of deformation likely extended westward beyond the limits of the sidehill exposure so that we were likely to expose faulted and/or folded sediments in the trench. We anticipated that the site was limited by the locations of occupied buildings at the eastern end of the property. Thus, there was a possibility that we would not get complete overlap with the side-hill excavation.

SE SHELL LANE TRENCH

This project consisted of a single, simple, fault normal excavation across a zone of deformation associated with the Portland Hills fault. The trench was oriented such that we could maximize the exposure given the available space. We excavated a 31 m-long, up to 4 m-deep, 1.2 m wide trench across the vacant property (Figure 7 and 8). We cleaned the trench walls and constructed a 1 x 1 m string grid across the north face of the exposure. We then flagged stratigraphic contacts, structures and potential radiocarbon sample sites. We then logged the information on gridded paper. Location references in the following discussion use station designations based on horizontal distances, for example station 12 refers to a location 12 m from the southwestern end of the trench.

Deposits

The trench exposed a sequence of medium- to fine-sand capped silt to clay deposits (Figure 7). Packages of sand to clayey silt pairs (Figure 9) were identified within the exposure. We defined individual beds that consist of basal medium to fine, massive to moderately laminated sands that fine upward to a relatively thin fine silt to clay. The sand bed thicknesses

range from less than 15 cm to more than 70 cm thick. The overlying fine-grained deposits are generally less than 20 to 30 cm thick and in places are discontinuous. Contacts between the top of the upper fine grain "cap" of a bed pair and the overlying bed pair are generally sharp.

Figure 8 - Photograph looking to southwest along the surface of the SE Shell Lane trench. Photograph taken after hydraulic shores removed prior to backfilling.

We identified at least 9 individual groups of paired sedimentary beds in the lower approximately 2 m of the trench (Units 12 to 4). The upper 2 m of the trench consists of massive, non-bedded clay and silt (Unit 3), overlain by a clay to clay loam (Unit 2). Rhythmites (Units 4 and 5) directly underlying Unit 3 are difficult to identify as there are is little variation in grain-size within these units between them and Unit 3. The northeastern lateral extent of Units 4 and 5 were difficult to discern for this reason.

Unit 2 is relatively flat lying and unconformably overlies the older deposits. The entire sequence is capped by a 30 to 60 cm thick chaotic clayey silt deposit (Unit 1) which we interpret to be human-derived fill.

Deposits similar to those we document in the SE Shell Lane trench and at the previous investigation sites have been described elsewhere in the Columbia and Snake River basins of eastern and central Washington and northernmost Oregon as rhythmites, typically characterized by fining upwards beds of contrasting grain size (for example, Atwater, 1984; Benito and

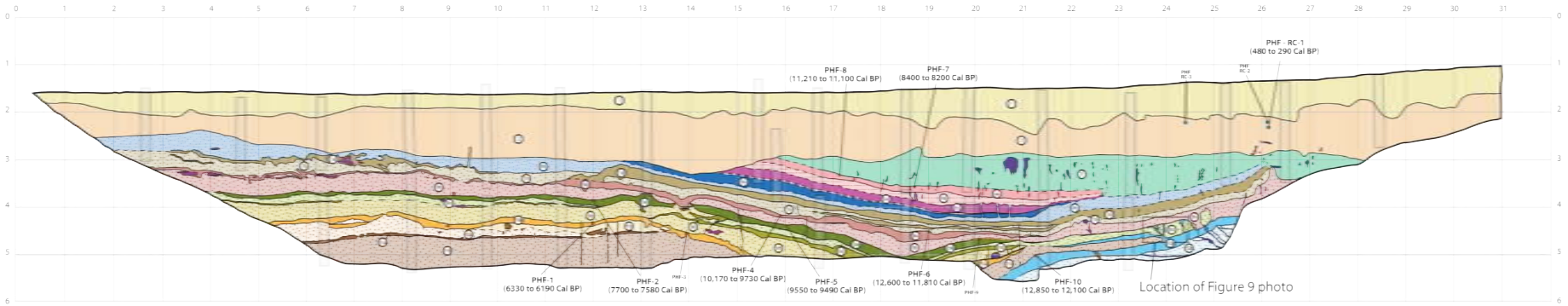

Disturbed zone (fill). Clayey silt with small lenses of coarse sand and exotic gravel. Also contains glass, plastic, and metal. Basal contact is undulatory and sharp. Some charcoal and baked soil.

B horizon?. Clay loam to clay. 90 to 100 cm in thickness. Structure is massive to weak. Contact is gradational (20 to 40 cm).

Clay and silt. Up to 100 cm thick. Top 30 to 50 cm convoluted with weak to moderate structure. Lower portion of unit is massive clay. Basal contact is gradational (10 to 30 cm) and faint.

Clay. Up to about 20 to 30 cm thick. Upper portion of unit (4a) has higher clay content. Lower portion of unit (4b) contains gray silty clay with numerous fractures. Basal contact of unit is gradational.

Clay. Up to about 20 to 30 cm thick. Upper portion of unit (4a) has higher clay content. Lower portion of unit (4b) contains gray silty clay with numerous fractures. Basal contact of unit is gradational.

Unit 6a is sandy silt and clay. Becomes clayier to the north. Unit 6 ranges from 40 to 70 cm thick. Unit 6b is massive fine sand. Medium sand near base of unit. Basal contact is undulatory and sharp.

Unit 7a is sandy silt and clay. At the southern 11.5 m of the trench, unit 7a is irregular, undulatory and less than 10 cm thick. To the north, unit 7a is thicker (20 to 30 cm) and less distorted. Unit 7b is a fine sand. Total thickness of unit 7 is about 30 to 50 cm. Unit becomes finer grained to the north. Base of unit is sharp and undulatory.

Unit 8a is sandy silt and clay. Unit 8a thins abruptly within the southern 11 m of the trench and absent in the northern 10 m of the trench. Unit 8b is fine sand. Total unit thickness varies from 15 to 40 cm.

Unit 9a is a thin (up to 15 cm thick) clayey silt in the southern part of trench to silty clay toward north. Unit 9a pinches out at about 22 m in the northern part of the trench. Unit 9b is a discontinuous, laminated fine sand. Unit 9c is a thin, discontinuous silty clay. The unit also pinches out at about 22 m in the northern part of the trench. Unit 9d is a 20 to 30 cm-thick fine sand layer. It also pinches out about about 22 m in the northern part of the trench. Basal contact of the unit is sharp and undulatory.

Unit 10a is a silty clay to clayey silt that is approximately 5 to 15 cm thick. Unit 10a pinches out at about 22 m in the northern part of the trench. Unit 10b is a fine- to medium-grained laminar sand. Individual beds are approximately 1 to 4 cm thick. Cross-bedding occurs between 8 to 9 m.

Unit 11a is a silty clay to clayey silt that is approximately 3 to 8 cm thick. Unit 11a pinches out at about 14 m in the northern part of the trench. Unit 11b is a fine- to medium-grained massive to laminar sand. This unit pinches out at about 25 m. Individual beds are approximately 1 to 4 cm thick.

Unit 12a is a silty clay to clayey silt that is approximately 10 to 20 cm thick. Unit 12a is only exposed between 21.5 and 26 m. There is an appearance of flow within this unit, such as dikes and sills (between 22.5 and 25 m). Fractures (between 24.5 and 26.5 m) extend through unit but do not extend into overlying deposits.Unit 12b is a fine- to medium-grained massive sand.

Radiocarbon bulk sample. Age estimates are calibrated ages before present.

Figure 7 - Map of deposits and strucures exposed in northwest wall of SE Shell Lane trench.

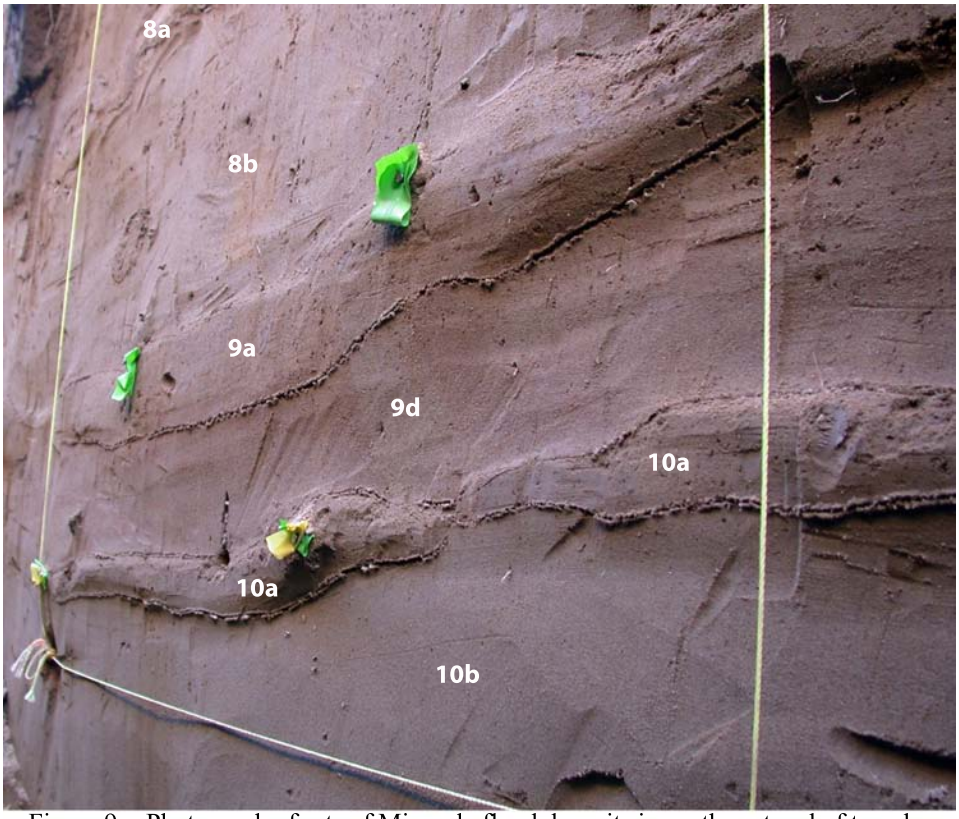

Figure 9 - Photograph of sets of Missoula flood deposits in southwest end of trench. View to southwest of medium- to fine-grained sands (Unit10b) overlain by fine silt and sand (Unit 10a). This group of sediments is overlain by another flood sequence of medium- to fine-grained sand (Unit 9d) and fine silt and sand (Unit 9a). Another flood package (Units 8b and 8a) occur in the top of the image. Vertical strings are 1 m apart.

O'Connor, 2003; O'Connor and Baker, 1992; Smith, 1993). These beds are the products of episodes of inundation by cataclysmic floods originating from late Pleistocene glacial Lake Missoula in western Montana. The rhythmic appearance of the deposits likely attests to the repeated periods of inundation that scoured much of central Washington and redeposited that material elsewhere downstream. Over a period of several thousand years, principally from about 17 to 12 kyr, as many as 89 floods have been recorded in Lake Columbia in northern Washington (Atwater et al., 2000, Benito and O'Connor, 2003). Perhaps as many as 40 of these floods backfilled the Willamette Valley as far as 250 km south of Portland (Minervini et al. 2003). The timing of individual flood events is not well-constrained but they appear to be separated by decades (Atwater et al., 2000; Clague et al., 2003, Benito and O'Connor, 2003). Minervini et al., 2003 provide a map showing the distribution, depth and type of deposits associated with Missoula floods in the Willamette Valley. They estimate the greatest depth of flooding in the valley to be about 122 m. At the SE Shell site the water depth would be in excess of 50 m. These beds are likely slackwater sediments formed as low velocity flood waters deposited fine-grained material in the Willamette River tributary to the Columbia River.

Structure

The overall structure exposed in the length of the trench is that of a broad, open syncline and anticline pair. We estimate the wavelength of the fold to be on the order of more than 20 m and the amplitude to be less than 3 m. The fold is truncated by Unit 2 deposits.

Except for a zone between stations 11 and 17, the southwestern portion of the trench was essentially devoid of fractures or faults. Within that portion of the trench, a zone containing thin, nearly vertical fractures in deposits older than Unit 9d are located between stations 12 and 13. Between stations 14 to 16.5 features appear to be clay-filled injection fractures or dikes. Several of them extend from as low as the base of the trench up into Unit 7b. However, several fractures

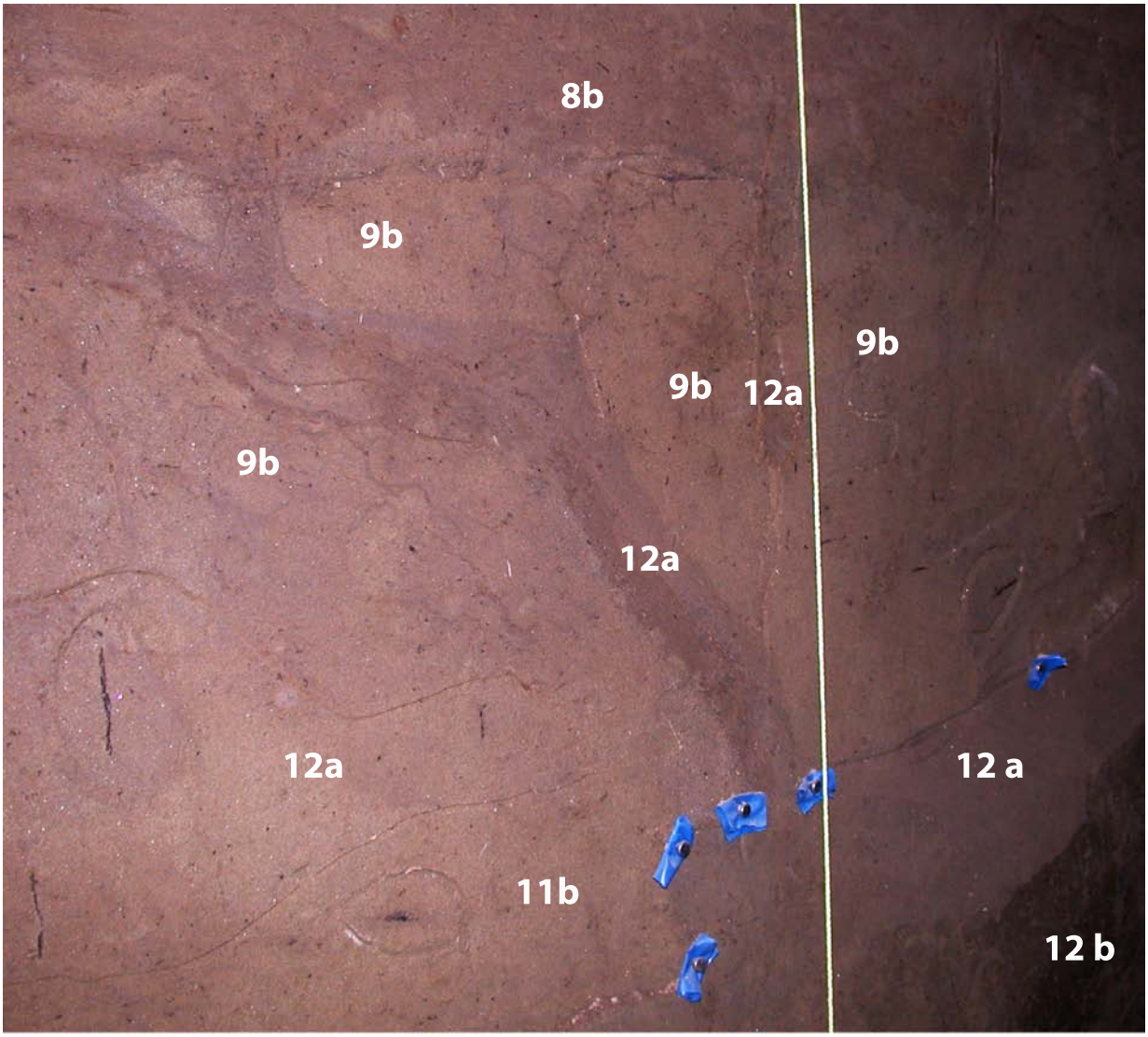

Figure 10 - View in lower northeast end of trench of fractured sands. Refer to Figure 6 for detailed map of trench between 24.5 and 26. 5 m. Vertical string is approximately 1 m long.

are discontinuous and do not extend downward beyond the base of the trench but appear to sole into one of the dominantly clay units such as Unit 10a between stations 14 and 15. The fractures located between stations 14 and 15.2 extend through several rhythmite packages suggest but not through overlying deposits. For example, a prominent, near vertical fracture at station 15 to 15.2 appears to postdate deposition of Units 10a, 9 and 8 but does not extend into Unit 7. Between stations 9 and 10, about 1.5 m below the ground surface, we document at sand-filled dike that intrudes into Unit 2. The dike extends no more than about 20 cm into the unit. It truncates abruptly within that unit. The dike appears to originate from Unit 7b. With the exception of a few small (< 20 cm wide, 5 cm thick) clay pods in the northeastern end of the trench (between stations 25.5 and 27.5) this is the only evidence for deformation we documented in the younger, upper deposits.

Fracture density and number increase toward the northeastern end of the trench (Figure 7). They appear to coincide with a portion of the synclinal structure between stations 20 and 26. A zone of fractures and possible soft-sediment injection feature occurs between stations 20 and 21 in the lower 1 m of the trench. Most conspicuous is a dike and sill feature that appears to originate within Unit 10a. It cross-cuts Unit 9 as a dike and then terminates at the base of Unit 8b where it extends laterally over a distance of about 1 m. Within that same trench width, near-vertical dikes, originating in Unit 6b cross overlying Units 6a and 5. The dikes contain medium-sand that is similar to that in Unit 6b.

A closely spaced series of clay-filled fractures, between stations 23 and 25, occur within Unit 12b, rarely within Unit 12a and not in younger units. Although the fractures range in dip from near vertical to near horizontal, they consistently dip toward the north. Within that same span of the trench, another group of fractures cross units 12 and 9b. These fractures terminate against the base of Unit 8b, and in at least one instance appear to be emplaced laterally against the base of 8b. This would suggest that Unit 8b existed at the time of dike formation. These fractures are more steeply oriented than the fractures found within Unit 12 a and b, however, they also consistently dip toward the north.

We also document discontinuous medium to dark brown clay filled fractures and pods throughout Unit 3 and, to a lesser extent, within Units 5b and 4a, b). These features (Figure 7) are near vertical and range from very small (< 5 cm in diameter) to relatively large (> 25 cm wide, ≥ 50 cm thick). Although they do not form continuous fractures, they occur in relatively narrow bands which suggests fracture-like behavior. Some very small clay-filled fractures were observed within the base of Unit 2 near the northeastern end of the trench (stations 25.8 to 27.2).

Near the base of the trench we observed a single, approximately 10 cm thick clay-filled fracture that crosses Unit 12 a and b but is truncated against the base of Unit 11b (Figure 7).

Age of Deposits

Estimation of the age for the deposits in the SE Shell Lane trench proved to be problematic. They were devoid of macroscopic detrital charcoal or other organic materials suitable for radiocarbon analysis. In hindsight, the lack of datable materials is not completely surprising although disappointing. The flood deposits are likely long-travelled and are reworked from older materials, including bedrock and prior flood deposits, originating from far upstream within the Channelled Scablands area of central Washington. The recurrence of the floods, on

the order of decades, likely prohibited significant accumulations of forests that would be the source of large woody debris. Additionally, the percentage of organics relative to the inorganic sediment content of the deposits is likely miniscule, especially in a location so far downstream of the source. During the course of the floods most macroscopic organic materials were likely crushed and abraded into microscopic particles.

In lieu of datable macroscopic samples we collected bulk samples primarily from within the fine-grained silty clay caps of the individual rhythmite beds. This might provide a maximum limiting age for the youngest part of an individual flood event. The samples were submitted to Paleo Research Institute, a company with expertise in identifying suitable materials for radiocarbon analysis related to archaeobotany research. They examined each sample for microscopic dateable materials. All samples were found to be devoid of such materials. As a last resort we submitted the samples to Beta Analytic for AMS analysis with the objective of extracting a radiocarbon date from the chelated organic materials found within the silt and clay matrix (Table 1).

The radiocarbon analysis provides a mixed range of calibrated ages for the sediments in the lower half of the trench that we interpret to be Missoula flood deposits (Table 1). The ages range from approximately 13,000 yr BP (PHF-TL10) near the base of the trench in Unit 12a to as young as ca. 6,200 yr BP (PHF-TL1) in Unit 10a also near the base. The ages are not stratigraphically consistent, i.e, with younger ages located within deposits found progressively higher in the section. That the ages might be mixed is not surprising given that there could be considerable mixing of various aged deposits from multiple sources from floods. Benito and O'Connor (2003) also found stratigraphically discordant ages, however, the ages were not inconsistent with the accepted range of ages for the Missoula floods. It is inconceivable that the youngest ages we derived from the rhythmite beds in the trench and interpret to be Missoula-aged flood deposits can be as young as Holocene given that were are glacially-derived during the glacial maximum. Other anomalously young ages include PHF-TL2 (Unit 9a, ca. 7,600 yr BP), PHF-TL5 (Unit 9a, ca. 9,500 yr BP) and PHF-TL7 (Unit 4a, ca. 8,300 yr BP). In more than one instance and inconsistency in ages occurs within a single unit. For example, Unit 8a has two sample ages, PHF-TL6 provides a range of ca. 12,000 yr B.P. to ca. 12,600 yr BP while PHF-TL4 provides an age range of approximately 9,700 yr BP to 10,200 yr BP. Unit 4a yields a range of ages from about 11,200 yr BP (PHF-TL8) to about 8,400 yr BP (PH-TL7).

The older ages (ca. 12,000 yr BP) for the deposits are at the younger end of the accepted range of ages for the Missoula flood deposits (Benito and O'Connor, 2003; Waitt, 1985). The anomalously young ages likely represent contamination of the bulk sample by younger material likely derived through pedogenesis, down-ward propagating fractures and cracks or groundwater. We cannot view these ages with much confidence given the anomalous and conflicting data they provide. We consider the older ages to provide evidence that the deposits are likely flood-related sediments related to the latter portion of the Missoula flood sequence.

A single detrital charcoal sample date from Unit 2, which unconformably overlies the flood deposit sequence, provides an age of 480 to 290 yr BP (PHF-RC1). The sample was located near the top of the deposit. We found no evidence for deformation of this unit however, a single sand dike intrudes into the base of the unit (Figure 7, station 9). Thus, the age estimate provides a minimum limit to the timing of the the most recent deformation at the site.

Deformation Events

Direct evidence for faulting is absent in the SE Shell Lane trench is absent, however, we do believe that sufficient evidence exists to conclude that multiple deformation events have occurred within the Missoula flood deposits. The entire sequence of Missoula flood deposits exposed in the trench is gently folded (Figure 7). Folding only becomes slightly more progressive with depth suggesting more deformation in older units (Figure 11). We consider the oldest event to be represented by an unconformity between Units 10 and 9 and more steep dips in Unit 10 (station 20) than the overlying deposits within the northeast hinge of the synclinal fold. At the northeast end of the trench (stations 23 to 26) a series of clay-filled fractures occur within Unit 12 but do not extend into Unit 9. Additionally, between stations 11 and 13, vertical fractures terminate at the base of Unit 9.

A second deformation event is represented by erosion of Unit 10a against Unit 9 at station 21. In addition, a series of fractures and sills occur within Units 12 through 9 that do not appear to propagate upward into younger units. At stations 21.5 to 25, material consistent with Unit 12a appears to be injected into Unit 9b as a series of dikes and as a sill that lies at the base of that unit and at the top of Unit 11b (Figure 7). Another fracture and sill-like structure occur at station 20 to 21. It appears to contain material from Unit 10a that has been injected into the base of Unit 8b and over the top of Unit 9a.

Another possible event is represented by another unconformity that occurs between Units 7 and 8 (station 19 to 21). This coincides with a younger set of fractures that occur primarily within the younger sequence of deposits (Units 5 through 3) and include clay-filled fractures and pods as well as sand-filled fractures that extend from Unit 6 through Unit 5b into the base of Unit 4b.

A single, prominent soft sediment dike intrudes into the base of Unit 2 (station 9.5). In addition, a few small clay filled fractures (station 25.5 to 27.5) occur in the base of the unit. The clay-filled features in underlying Unit 3 do not coincide with any of the clay features in Unit 2.

We attempted to combine the logs from both the side-hill excavation at RMS and the SE Shell Lane trench to create a longer stratigraphic section. The two exposures were separated by about 15 m and appeared to overlap, however, without clear connection between the two there are likely errors in the correlation. We attempted to tie obvious sedimentary sequences between the two trenches (Figure 11). A similar style of folding is apparent between the two exposures with gentle, open folding characteristic of both. Near the overlap between the two trenches, where fracturing becomes more pronounced, the folding becomes slightly more irregular and correlation becomes more problematic.

DISCUSSION

The SE Shell Lane trench exposes evidence for multiple deformation events within the Missoula flood deposits. This, combined with geophysical evidence from North Clackamas Park and nearby Rowe Middle School for pronounced offset of Miocene Columbia River Basalts and progressive deformation of overlying sediments along the projected Portland Hills fault provides compelling evidence that the deformation within the trench is related to movement on the fault.

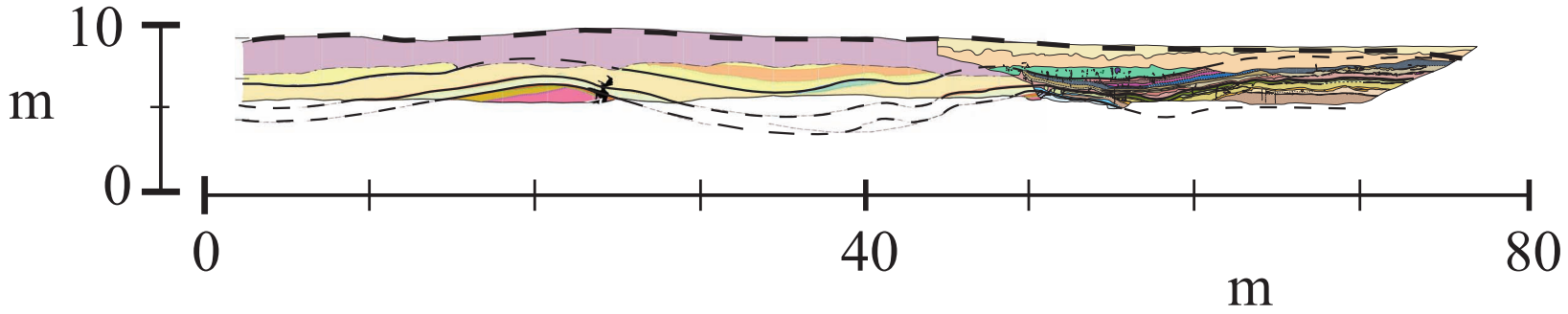

Figure 11 - combined geologic logs from Rowe Middle School and SE Shell Lane with projected topography (from Glandstone 7.5° sheet). Superimposed lines show inferred contact correlations between trenches. The overall shortening over the length of the combined trenches is about 4 to 5 m or about 6 to 7%.

However, no conclusive evidence for primary surface rupture is evident from the excavation. Without evidence for primary displacement of the Missoula deposits it is permissive that the deformation is shaking-related and possibly due to another area source.

During the time that the trench was open there was concern that the northeastern end of the excavation was near to but had not exposed a fault. Folding and fractures were more pronounced in this end of the trench. We were unable to excavate further due to constraints from underground pipes and surface structures.

One potential cause of the warping and fracturing in the flood deposits is soft-sediment deformation resulting from loading of progressively younger deposits or by dewatering of the saturated materials. We consider this mechanism unlikely because the sediments have undergone shortening suggesting horizontal compression. Additionally, the folding occurs throughout the section and is not isolated to just one or a few beds.

ACKNOWLEDGMENTS

Funding for this proposal was provided from the U.S. Geological Survey National Earthquake Hazards Reduction Program Award Number 03HQGR0020. We wish to thank Rowe Middle School for access to the school property. We also thank the Cheregino family for allowing us to conduct geophysical surveys within their farm between the Rowe Middle School and North Clackamas Park. Finally, we thank Jerry Black of the Oregon Department of Geology and Mineral Industries for his help in this project.

REFERENCES CITED

Atwater, B.F., Smith, G.A., and Waitt, R.B., 2000, The Channeled Scabland: Back to Bretz?: Comment and Reply, Geology, v. 28, p. 573-576.

Beeson, M.H., Fecht, K.R., Reidel, S.P., and Tolan, T.L., 1985, Regional correlations within the Frenchman Springs Member of the Columbia River Basalt Group: New insights into the middle Miocene tectonics of northwestern Oregon: Oregon Geology, v. 47, p. 87-96.

Beeson, M.H., and Tolan, T.L., 1990, The Columbia River Basalt Group in the Cascade Range: A Middle Miocene reference datum for structural studies: Journal of Geophysical Research, v. 95, p. 19547-19559.

Beeson, M.H., Tolan, T.L., and Anderson, J.L., 1989, The Columbia River Basalt Group in western Oregon; geologic structures and other factors that controlled flow emplacement patterns: Geological Society of America Special Paper 239, p. 223-246.

Beeson, M.H., Tolan, T.L., and Madin, I.P., 1991, Geologic map of the Portland quadrangle, Multnomah and Washington counties, Oregon and Clark county, Washington, Oregon Department of Geology and Mineral Industries.

Benito, G., and O'Connor, J.E., 2003, Number and size of last-glacial Missoula floods in the Columbia River valley between the Pasco Basin, Washington, and Portland, Oregon, Geological Society of America Bulletin, v. 115, p. 624-638.

Blakely, R.J., Wells, R.E., Tolan, T.L., Beeson, M.H., Trehu, A.M., and Liberty, L.M., 2000, New aeromagnetic data reveal large strike-slip (?) faults in the northern Willamette Valley, Oregon: Geological Society of America Bulletin, v. 112, p. 1225-1233.

Blakely, R.J., Wells, R.E., Yelin, T.S., Madin, I.P., and Beeson, M.H., 1995, Tectonic setting of the Portland-Vancouver area, Oregon and Washington: Constraints from low-altitude aeromagnetic data: Geological Society of America Bulletin, v. 107, p. 1051-1062.

Bott, J.D.J., and Wong, I.G., 1993, Historical earthquakes in and around Portland, Oregon: Oregon Geology, v. 55, p. 116-122.

Clague, J.J., Barendregt, R., Enkin, R.J., and Foit, F.F., 2003, Paleomagnetic and tephra evidence for tens of Missoula floods in southern Washington, Geology, v. 31, p. 247-250.

Hemphill-Haley, M., Liberty, L.M., and Madin, I.P., 2002, Source Characterization Study of the Portland Hills Fault, Portland Metropolitan Area, Oregon, Volume Final Report for National Earthquake Hazards Reduction Program Award Number 00HQR0023, p. 16.

Hunter, J.A., Pullan, S.E., Burns, R.A., Gagne, R.M., and Good, R.L., 1984, Shallow seismic reflection mapping of the overburden-bedrock interface with the engineering seismograph - Some simple techniques: Geophysics, v. 49, p. 1381-1385.

Johnson, S.Y., Dadisman, S.V., Childs, J.R., and Stanley, W.D., 1999, Active tectonics of the Seattle fault and central Puget Sound, Washington - Implications for earthquake hazards: Geological Society of America Bulletin, v. 111, p. 1042-1053.

Liberty, L.M., Trehu, A.M., Blakely, R.J., and Dougherty, M.E., 1999, Integration of high-resolution seismic and aeromagnetic data for earthquake hazards evaluations: an example from the Willamette Valley, Oregon: Bulletin of the Seismological Society of America, v. 89, p. 1473-1483.

Madin, I.P., 1990, Earthquake-hazard Geology Maps of the Portland Metropolitan area, Oregon, Oregon Department of Geology and Mineral Industries.

Madin, I.P., and Hemphill-Haley, M.A., 2001, The Portland Hills fault at Rowe Middle School: Oregon Geology, v. 63, p. 47-49.

Madin, I.P., Priest, G.R., Mabey, M.A., Malone, S., Yelin, T.S., and Meier, D., 1993, March 25, 1993, Scotts Mills earthquake - Western Oregon's wake-up call: Oregon Geology, v. 55, p. 51-57.

Magill, J., Cox, A., and Duncan, R., 1981, Tillamook volcanic series: further evidence for tectonic rotation of the Oregon Coast Range: Journal of Geophysical Research, v. 86, p. 2953-2970.

Minervini, J.M., O'Connor, J.E., and Wells, R.E., 2003, Maps showing inundation depths, ice-rafted erratics, and sedimentary facies of late Pleistocene Missoula floods in the Willamette Valley, Oregon, U. S. Geological Survey, Open-File Report, OF 03-0408.

Pratt, T.L., Odum, J., Stephenson, W., Williams, R., Dadisman, S., Holmes, M., and Haug, B., 2001, Late Pleistocene and Holocene tectonics of the Portland Basin, Oregon and Washington, from high-resolution seismic profiling: Bulletin of the Seismological Society of America, v. 91, p. 637-650.

Steeples, D.W., and Miller, R.D., 1998, Avoiding pitfalls in shallow seismic reflection studies: Geophysics, v. 63, p. 1213-1224.

Swanson, R.D., McFarland, J.B., Gonthier, J.B., and Wilkinson, J.M., 1993, A description of hydrogeologic units in the Portland basin, Oregon and Washington, USGS Water-Resources Invest. Rept. 90-4196, p. 56.

Waitt, R.B., 1985, Case for periodic, colossal jokulhloups from Pleistocene glacial Lake Missoula: Geological Society of America Bulletin, v. 96, p. 1271-1286.

Walsh, T.J., Korosec, M.A., Phillips, W.M., Logan, R.L., and Schasse, H.W., 1987, Geologic map of Washington, southwest quadrant, Washington Division of Geology and Earth Resources Geologic Map GM-34.

Wells, R.E., 1990, Paleomagnetic rotations and the Cenozoic tectonics of the Cascade Arc, Washington, Oregon, and California: Journal of Geophysical Research, v. 95, p. 19,409-19,417.

Wells, R.E., Weaver, C.S., and Blakely, R.J., 1998, Fore-arc migration in Cascadia and its neotectonic significance: Geology, v. 26, p. 759-762.

Werner, K., Nabelek, J., Yeats, R., and Malone, S., 1992, The Mount Angel fault: Implications of seismic-reflection data and the Woodburn, Oregon, earthquake sequence of August 1990: Oregon Geology, v. 54, p. 112-117.

Wong, I., Silva, W., Bott, J., Wright, D., Thomas, P., Gregor, N., Li, S., Mabey, M., Sojourner, A., and Wang, Y., 2000, Earthquake Scenario and Probabilistic Ground Shaking Maps for the Portland, Oregon, Metropolitan Area, State of Oregon, Department of Geology and Mineral Industries, p. 11 map sheets.

Wong, I.G., 1997, The historical earthquake record in the Pacific Northwest: Applications and implications to seismic hazard assessment, *in* Neuendorf, K.K.E., ed., Earthquakes-Converging at Cascadia, Association of Engineering Geologists Special Publication 10, p. 19-36.

Wong, I.G., Hemphill-Haley, M.A., Liberty, L.M., and Madin, I.P., 2001, The Portland Hills fault: an earthquake generator or just another old fault?: Oregon Geology, v. 63, p. 39-50.

Yeats, R.S., Graven, E.P., Werner, K.S., Goldfinger, C., and Popowski, T.A., 1996, Tectonics of the Willamette Valley,

Oregon, *in* Rogers, A.M., et al., ed., Assessing earthquake hazards and reducing risk in the Pacific Northwest; U. S. Geological Survey Professional Paper 1560, p. 183-222.

Yelin, T.S., and Patton, H.J., 1991, Seismotectonics of the Portland, Oregon, region: Bulletin of the Seismological Society of America, v. 81, p. 109-130.

Table 1 - Radiocarbon Data for the Portland Hills Fault trench at SE Shell Lane.

Trench Sample No.	Laboratory Sample No.	Sample Material	Stratigraphic Unit	$\delta^{13}C$ (‰)	Lab-reported conventional age (^{14}C yr BP at 1σ)[b]	Calibrated age (yr BP at 2σ)[c\]
PHF-RC1	Beta - 195003	organic sediment	2	-24.8	310 +/- 40	480 to 290
PHF-TL7	Beta - 195000	organic sediment	4a	-24.1	7520 +/- 50	8400 to 8200
PHF-TL8	Beta - 195001	organic sediment	4a	-24.3	9730 +/- 50	11210 to 11100
PHF-TL4	Beta - 194997	organic sediment	8a	-24.5	8860 +/- 50	10170 to 9730
PHF-TL6	Beta - 194999	organic sediment	8a	-24	10290 +/- 50	12600 to 12500 and 12370 to 11810
PHF-TL2	Beta - 194996	organic sediment	9a	-23.1	6790 +/- 50	7700 to 7580
PHF-TL5	Beta - 194998	organic sediment	9a	-24	8530 +/- 40	9550 to 9490
PHF-TL1	Beta - 194995	organic sediment	10a	-23.7	5480 +/- 50	6330 to 6190
PHF-TL10	Beta - 195002	organic sediment	12a	-24	10490 +/- 50	12850 to 12290 and 12250 to 12100

a) Reported ages are corrected for \δ13C and include a laboratory error multiplier of 1.0 in reported laboratory uncertainty; samples analyzed by Beta Analytic, Inc. (radiocarbon years before present; "present"=1950AD) b) Read -25 as value of 25% measured for 13C/12C ratio; NA = not available. c) Calibrated using Stuiver and Reimer (1998).